NIH Public Access
Author Manuscript

A Novel CNS-Restricted Isoform of the IL-1R Accessory Protein Modulates Neuronal Responses to IL-1

Dirk E. Smith[1,*], **Brian P. Lipsky**[1], **Chris Russell**[2], **Randal R. Ketchem**[3], **Jacqueline Kirchner**[1], **Kelly Hensley**[1], **Vincent Boissonneault**[4], **Marie-Michèle Plante**[4], **Serge Rivest**[4], **Yangyang Huang**[5], **Wilma Friedman**[5], and **John E. Sims**[1]

[1]Department of Inflammation Research, CHUL Research Center, Sainte Foy, Quebec, Canada

[2]Department Molecular Sciences, CHUL Research Center, Sainte Foy, Quebec, Canada

[3]Department Protein Sciences, Amgen, Seattle, Washington, 98119, USA, CHUL Research Center, Sainte Foy, Quebec, Canada

[4]Department Laboratory of Molecular Endocrinology, CHUL Research Center, Sainte Foy, Quebec, Canada

[5]Department of Biological Sciences, Rutgers University, Newark, New Jersey 07102.

SUMMARY

IL-1 has multiple functions in both the periphery and the central nervous system (CNS) and is regulated at many levels. We identified a novel isoform of the IL-1R Accessory Protein (termed AcPb) that is expressed exclusively in the CNS. AcPb interacted with IL-1 and the IL-1 receptor but was unable to mediate canonical IL-1 responses. AcPb expression, however, modulated neuronal gene expression in response to IL-1 treatment in vitro. Animals lacking AcPb demonstrated an intact peripheral IL-1 response and developed experimental autoimmune encephalomyelitis (EAE) similarly to wild type mice. AcPb-deficient mice were instead more vulnerable to local inflammatory challenge in the CNS and suffered enhanced neuronal degeneration as compared to AcP-deficient or wild type mice. These findings implicate AcPb as an additional component of the highly regulated IL-1 system and suggest it may play a role in modulating CNS responses to IL-1 and the interplay between inflammation and neuronal survival.

INTRODUCTION

The IL-1 cytokines IL-1α and IL-1β induce cellular responses through a widely expressed receptor complex comprised of the type I IL-1R and the IL-1R Accessory Protein (AcP) (Sims, 2002). The AcP receptor subunit is also used by the IL-1F6, IL-1F8 and IL-1F9, and IL-33 receptors (Ali et al., 2007; Chackerian et al., 2007; Palmer et al., 2008; Towne et al., 2004). Ligation of the IL-1 receptor complex leads to recruitment of intracellular signaling molecules mediated by conserved cytoplasmic Toll-IL-1R (TIR) domains. These signaling events underlie IL-1's ability to regulate host defense and tissue homeostasis in virtually every organ of the body. The excessive or prolonged action of IL-1, however, can lead to

[*]correspondence: smithde@amgen.com.

destructive inflammation and contribute to disease. IL-1 has been shown to play a causative or contributing role in hereditary fever syndromes, gout, rheumatoid and systemic-onset juvenile arthritis, and type II diabetes, and there are strong suggestions of involvement in osteoarthritis, ischemia-reperfusion injury, neuropathic and inflammatory pain, and Alzheimer's Disease. Consequently, multiple mechanisms have evolved to regulate IL-1 activity. IL-1 is strongly induced at the transcriptional level in response to innate inflammatory stimuli and the processing of IL-1β protein from precursor to active form and its secretion from the cell are regulated processes. Subsequent to the generation of mature, active IL-1, signaling can be attenuated by an inactive ligand analog (IL-1ra) and an inhibitory soluble receptor (IL-1R type 2). The latter acts by decoying not only the IL-1 cytokine but also the essential receptor subunit, AcP (Sims and Smith, 2003). In this communication, we describe an additional, more subtle form of regulation. We have found a novel splice variant of AcP, termed AcPb, which is expressed in a CNS-specific manner and which interferes with some, but not all, IL-1 activities and thus modulates the effects of IL-1 in the brain.

RESULTS

Discovery of AcPb, a novel IL-1R AcP splice isoform with a variant TIR domain

We identified a novel open reading frame in human genomic DNA sequence with similarity to members of the IL-1R family. Subsequent cloning of the full-length cDNA from both human and mouse revealed a novel isoform of AcP that we have termed AcPb. **Figure 1a** illustrates the alternative splicing by which the prototypical AcP C-terminal exon 12 is skipped and the novel exon is utilized. Shown in **Figure 1b** is a sequence alignment of the polypeptides encoded by exons 11-12 from AcP and the AcPb isoform. The C-terminus encoded by exon 12b in AcPb has only 35% amino acid identity with that encoded by the classic AcP exon 12. It shares motifs, however, such as box 3 (FWK) that are conserved in all TIR domains. In addition, AcPb exon 12b encodes approximately 140 amino acids of additional sequence C terminal to the TIR domain that has no homology to other protein sequences and is of unknown function. Similar C-terminal extensions following the TIR domain are found on a subset of other IL-1R family proteins, namely SIGIRR, TIGIRR and IL-1RAPL (TIGIRR-2), however the level of sequence identity among them is low.

Crystal structures have been determined for the TIR domains of TLR1 and TLR2 (Xu et al., 2000) as well as the orphan IL-1R family member IL-1RAPL (Khan et al., 2004). We used the latter on which to model the TIR domains of AcP and AcPb and adopted the same convention for annotation of secondary structure. The AcP TIR domain (amino acids 401-553) is predicted to contain a central five-stranded beta-sheet surrounded by five alpha-helices (**Figure 1c**). The AcPb sequence was easily modeled onto the same structure and was remarkably similar to that of AcP, including conservation of the EE loop (approximately amino acids 527-534), previously implicated as an important site for MyD88 recruitment (Li et al., 2005; Radons et al., 2003). The only significant predicted difference between AcP and AcPb is the disruption of the αD helix in AcPb, due predominantly to two proline substitutions at amino acids 508 and 510. Predicted electrostatics indicated a more negatively-charged surface on the face of the AcPb TIR domain made up of the βE strand

and the DD loop-αD helix region, as a consequence of the disruption of the helix (**Figure 1c, lower panel**). Overall, the computational modeling indicated that the AcPb cytoplasmic domain likely folds as a TIR domain similar to AcP, but with one area of substantial difference.

AcPb expression is restricted to the CNS

RNA expression profiling demonstrated that whereas human AcP is expressed in numerous tissues, the expression of the AcPb isoform is much more restricted to tissues derived from the CNS (whole brain, fetal brain, cerebellum and spinal cord) and is the more abundant isoform in these CNS tissues, with the exception of spinal cord (**Figure 2a**). AcPb message was undetectable or present at extremely low levels in multiple non-CNS-derived cell types and in various established cell lines including those of CNS origin, such as numerous glioblastoma and neuroblastoma-derived lines (*not shown*). Bronchial epithelial cells were the only non-CNS sample in which AcPb mRNA was detected; however, the expression level was 100-fold lower than AcP and approximately 30-fold lower than the level of AcPb mRNA in total brain RNA (*not shown*). The CNS-predominant expression pattern of AcPb was also observed among mouse tissues and cell lines (*not shown*). We next profiled the relative expression of AcP and AcPb mRNA across multiple anatomical regions of human adult brain. For comparison, the same analysis was done for both the neuron-specific gene, microtubule-associated protein 2 (MAP2) and the astrocyte-specific gene, glial fibrillary acidic protein (GFAP). As shown in **Figure 2b**, AcP and AcPb have slightly different patterns of relative brain expression. For example, AcP is much more enriched in the corpus callosum than AcPb. The AcPb expression pattern is more similar to that of MAP2 than that of GFAP, suggesting a more neuronal-restricted expression pattern. RT-PCR analysis of purified neurons, microglia and astrocytes also indicated a more neuron-restricted expression of AcPb, whereas abundant AcP mRNA was detected in all three cell types (Figure 2c and data not shown). *In situ* RNA hybridization was used to examine the location of expression in adult mouse brain sections with RNA probes specific for AcP or AcPb exon 12. As shown in **Figure 2d**, AcP and AcPb displayed overlapping patterns of expression that corresponded to areas of neuronal bodies throughout the gray matter. Collectively, these results suggest neuronal expression of AcPb throughout the brain. The mouse in situ hybridization data **and RT-PCR results** might suggest that AcP and AcPb are co-expressed in the same cells, rather than being expressed in different cells in the same anatomical areas, but we have been unable to raise the appropriate antibodies to prove this.

AcPb associates with IL-1R in an IL-1 dependent manner but is unable to recruit MyD88 and IRAK4

The AcPb variant conserves the extracellular domain required for interaction with IL-1R and IL-1 so we asked whether AcPb is able to form complexes with the type I IL-1R in a ligand-dependent manner. We utilized the IL-1R-positive, AcP-negative mouse T cell line EL4.16a that was stably transduced with either a control protein (GFP) or full-length AcP or AcPb. The surface expression of reconstituted AcP or AcPb was found to be similar in both lines (**Figure 3a**). As shown in **Figure 3b, (lanes 1-3)**, IL-1R was coimmunoprecipitated from both the AcP and AcPb-expressing lines but not in the control cells that lack AcP. Moreover, the recruitment of IL-1R was dependent on ligation with IL-1 as no IL-1R band was

detected in the lanes from non-treated cells (**Figure 3b, lanes 4-6**). Immunoblotting with an anti-AcP antibody confirmed that AcP and AcPb were both effectively immunoprecipitated even in the absence of IL-1. These results indicated that AcPb is capable of forming a ligand-dependent complex with IL-1R.

The proximal events that lead to IL-1-induced cellular responses involve the recruitment of specific adaptor and signaling molecules to the IL-1R:AcP complex. Two such molecules previously shown to be crucial for elicitation of IL-1 responses are the adaptor molecule MyD88 and the kinase IRAK4 (Burns et al., 2003; Huang et al., 1997; Jiang et al., 2003; Wesche et al., 1997a). Immunoprecipitation experiments with the IL-1-treated EL4 lines demonstrated that only the AcP-expressing cells are capable of recruiting MyD88 and IRAK4 following stimulation with IL-1 (**Figure 3c**). Although AcPb was able to associate with IL-1R under these IL-1-dependent conditions, it did not lead to the recruitment of these adaptor molecules.

AcPb is unable to mediate canonical IL-1 signaling responses in EL4 cells

Experiments were next performed to determine whether AcPb possesses autonomous signaling capacity in response to IL-1 in the mouse EL4 cells. As shown in **Figure 4a**, AcP-reconstituted, but not AcPb-reconstituted cells secreted IL-2, IL-5 and IL-6 in response to IL-1 treatment. In separate experiments, and consistent with previously reported results (Wesche et al., 1997b), the AcP-negative control EL4 cells were non-responsive to IL-1, demonstrating that these responses are AcP-dependent (*not shown*). The inability of AcPb to mediate IL-1-induced cytokine release was next shown to correspond to an inability to activate IL-1 signaling. IL-1 treatment led to the activation of p38, JNK, and ERK in the cells reconstituted with AcP, but not in the cells reconstituted with AcPb (**Figure 4b**). Sorbitol has previously been shown to induce p38 activation (Alpert et al., 1999) and when used as a control stimulus, led to activation of phosphorylated p38 in all three EL4 lines, indicating that AcPb expression does not lead to a general defect in cellular responsiveness but rather, consistent with an inability to recruit MyD88 and IRAK4, is unable to mediate these specific IL-1 responses.

AcPb effects on gene expression in virally reconstituted AcP$^{-/-}$ cortical neurons

We hypothesized that because the expression pattern of AcPb suggests a centrally localized function, AcPb-dependent IL-1 responses may manifest only in a CNS-related context. For example, AcPb may utilize adaptor molecules possessing the same restricted tissue expression as AcPb itself. We used a primary neuron culture system to explore this hypothesis. Cortical neuron cultures were established from C57BL/6 E17-E18 embryos and after 7-10 days the cultures were approximately 70-80% pure MAP2-positive neurons with active neurite outgrowth (**Figure 5a**). Some glial cells, including GFAP-positive cells were also present and represented approximately 20-30% of the culture. RT-PCR indicated that IL-1R, AcP and AcPb were all expressed in these cultures and all seemed to increase in expression as the cultures matured (*not shown*). In order to evaluate the specific contribution of AcP and AcPb towards responses to IL-1, reconstitution experiments were performed using neuronal cultures from *IL1rap* (AcP-null) E17.5 embryos. The *IL1Rap* targeted deletion eliminates two exons in the extracellular domain of AcP (as shown in **Figure 1a**)

and thus destroys the expression of all functional AcP isoforms (Cullinan et al., 1998). Based on the previously shown ability of lentivirus to infect non-dividing neurons (Blomer et al., 1997), cortical neurons from AcP$^{-/-}$ embryos were transduced in triplicate with lentiviral vectors expressing full-length AcP, AcPb, or CD25 as an unrelated control protein. A fourth population was transduced with equal amounts of both the AcP and AcPb vector in order to evaluate the effect of isoform co-expression. The infection conditions were shown to lead to vector-driven gene expression in neurons (not shown). Two days post-infection, cultures were stimulated with IL-1β for 4 or 16 hours and total RNA was harvested. RT-PCR analysis confirmed the reconstituted expression of specific receptor isoforms in each population (**Figure 5b**). Moreover, functional responsiveness was demonstrated by an IL-1-dependent increase in CCL2 expression in AcP-reconstituted cultures (**Figure 5c**).

In order to broadly survey the gene expression profiles of each of the IL-1 stimulated populations, RNA samples were analyzed on microarray chips containing approximately 45,000 gene probe sets. In the AcP-null cultures (control virus-transduced), when comparing untreated samples to IL-1 stimulated samples at either 4 or 16 hours, the observed gene expression changes were at the level of statistical noise, consistent with the AcP requirement for IL-1 signaling (**Figure 5d**). In contrast, many genes were induced in the AcP-reconstituted cultures stimulated with IL-1. Statistically significant ($p <0.05$) gene expression ratios for IL-1-treated versus untreated sample sets ranged from 1-2 fold up to 100-fold (the limit of the analysis dynamic range) and the specific genes regulated largely overlapped when comparing the 4 and 16 hour datasets (*not shown*). There was also significant overlap between the IL-1 induced genes in the AcP-reconstituted culture and genes induced by IL-1 in a previous study with wild type C57BL/6 cortical neurons (*not shown*), suggesting that transduced AcP mediated normal responses to IL-1 in this system. Some of the most robustly induced genes included chemokines such as CXCL1, CXCL10, and CCL2, as well as immune-related products such as TLR2 and TWEAK receptor (**Supplementary Table 1**). In contrast to the AcP-reconstituted culture, there were no genes consistently induced greater than 2-fold in the AcPb-reconstituted culture (**Supplementary Table 2**). Moreover, the few gene responses that reached statistical significance in AcPb samples were generally induced to similar levels in the AcP-reconstituted cultures. These results indicated that AcPb-reconstituted neuronal cultures may be capable of a limited IL-1 signaling response, although all of the gene responses were modest and none were unique to AcPb.

Analysis of the AcP + AcPb-reconstituted culture compared to AcP alone indicated that AcPb co-expression is capable of modulating AcP-dependent responses. A few genes showed slightly increased induction in the AcP + AcPb-reconstituted culture as compared to AcP alone, but all of the most highly induced transcripts were induced to similar levels in the culture with AcP alone, supporting the idea that no strong gene induction signal is specifically transduced through AcPb. Interestingly, there were two classes of AcP-dependent gene responses: those that were unaffected by AcPb co-expression (example: *GBP2* fold induction at 4 hours: AcP population, 36.8, AcP + AcPb population, 38.5) and those that were attenuated in the presence of AcPb (example: *ATF3* fold induction at 4 hours: AcP population, 22.4, AcP + AcPb population, 3.8). A summary of representative

genes in both of these classes is shown in **Table 1**. These results suggest that in the context of a neuronal culture AcPb co-expression may down-modulate some but not all AcP-dependent IL-1 responses.

Generation of AcPb-deficient mice

In order to better understand the specific function of the AcPb isoform we generated AcPb exon 12b knockout mice. A targeting vector was designed to delete only the unique exon 12b of the AcPb isoform while leaving all of the coding exons for classical AcP intact, as indicated in **Figure 1a**. Homozygous knockout animals were generated and backcrossed completely onto a C57BL/6 background. As shown in **Figure 6a**, expression of both AcP and AcPb was detected in wild type whole brain whereas, as expected, both were absent in brains from AcP-deficient animals. In contrast, only AcPb expression was disrupted in the brain of AcPb-deficient mice. **At the protein level,**, multiple AcP-related bands were detected in wild type brain by immunoprecipitation **and Western blotting**, including bands corresponding to full-length AcP and the slightly larger AcPb. We also detected smaller-sized bands, possibly corresponding to the soluble AcP mRNA variant that we have confirmed is expressed in the brain at the RNA level (*not shown*), however, proteomic analysis would be required to verify their identity. Control immunoprecipitations were performed with lysates from AcP- and AcPb-expressing EL4 cells. It is not clear why the receptors did not migrate exactly as the proteins in lysates from transfected EL4 cells however differential glycosylation may underlie some of this difference. The larger AcPb-sized band was uniquely absent in the brains from AcPb-deficient mice indicating that the exon 12b deletion **resulted in loss of this isoform but** did not interfere with protein expression of the other forms of AcP.

AcPb-deficient mice bred normally and were phenotypically normal. Staining of brain sections from eight week old AcP or AcPb knockout mice with Weil (to reveal myelin) and Thionine Nissl (to reveal cell bodies) did not reveal obvious abnormalities as compared to age- and gender-matched wild type controls (**Figure 6c**). We next demonstrated that peripheral responsiveness to IL-1 was still intact in AcPb-deficient mice. IL-6 induction in response to IL-1 was observed in splenocyte cultures from three independent mice from both wild type and AcPb knockout colonies (**Figure 6d**). In contrast, IL-1 was unable to induce IL-6 secretion from AcP-deficient splenocytes **(p value <0.01),** consistent with previous findings (Cullinan et al., 1998). All three cultures responded to LPS stimulation, indicating that cells from both knock-outs were still responsive to an alternative form of activation. Taken together, our results indicate that the AcPb exon 12b deletion selectively ablated the AcPb isoform while maintaining classic AcP expression and function.

The effects of pan-AcP and AcPb-specific deletion differ in peripherally- versus centrally-induced models of CNS inflammation

We examined the effect of complete AcP deficiency versus AcPb-specific deletion in two different models of immune-mediated CNS pathology. First, we evaluated both knockout strains in EAE, a model of peripherally-induced autoimmune-meditated CNS disease. Subcutaneous immunization with MOG_{35-55} in CFA resulted in 100% disease incidence in wild type C57Bl/6 mice (**Figure 7a**). In contrast, AcP-deficient mice were almost

completely protected from disease, with only 5% incidence of disease (1 of 18 mice) and a significant decreases both weight loss and clinical score compared to wild type mice (**Figure 7a-c**). AcPb knockout mice, however, had disease onset and incidence (**Figure 7a**) and disease progression (**Figure 7b and c**) similar to that of wild type controls. However at day 11 post-immunization, the AcPb-deficient mice did have a statistically significant increase in weight loss compared to wild type controls ($p<0.05$) (**Figure 7b**). We measured mRNA levels of several inflammatory mediators in the spinal cords of naïve mice and mice at day 20 post-immunization. As shown in **Figure 7d**, MOG$_{35-55}$ immunization led to significantly elevated levels of IL-1β and TNF in the spinal cords of wild type mice compared to naïve animals, as expected. IL-1β and TNF were comparably increased in the spinal cords of immunized AcPb-deficient mice, but not in AcP-deficient mice, compared to the respective naïve controls. These results correlated with the disease status in these mice. We also observed evidence of T cell-driven CNS inflammation, including increased levels of the Th1-associated transcription factor T-bet and the effector cytokine IL-17A, in immunized wild type and AcPb knockout mice, but not the AcP knockout mice, compared to naïve mice. Taken together, these results indicate that the absence of AcP is associated with profound protection from EAE, whereas loss of AcPb does confer the same protection.

Innate immune activation in the brain is not itself detrimental but can lead to neurotoxic consequences if not adequately regulated, such as, for example, in the context of glucocorticoid blockade. In such a model, it has been shown that the ensuing neurodegeneration in response to a single intracerebral bolus of LPS is in part dependent on IL-1, suggesting that in the absence of sufficient regulation of IL-1 activity signaling can lead to neuronal loss (Nadeau and Rivest, 2003). We used this experimental system to determine whether the regulatory effect of AcPb expression is associated with neuroprotection in the context of a local inflammatory response. LPS was infused into the brains of wild type, AcP- or AcPb-deficient mice (3-4 mice/group) and subsequent inflammatory response and neuronal damage was assessed by in situ hybridization for expression of IL-1β and the myelin constituent PLP, respectively, or by Fluoro-Jade (FJB) staining of degenerative neurons. Consistent with previous findings, LPS was shown to induce an inflammatory response in the brain as evidenced by induction of IL-1β mRNA within 24 hours, which was similar in all three lines of mice (**Figure 7e**). IL-1β mRNA was undetectable in the saline-treated animals (*not shown*). As shown in **Figure 7f-h**, LPS administration did not lead to observable demyelination or neuronal loss in either wild type or AcP-deficient animals. In contrast, at day 3, AcPb-deficient mice exhibited a clear and localized loss of expression of the myelin constituent PLP that was near, but distinct from, the LPS injection site. This decrease in PLP mRNA expression is frequently associated with a concomitant neurodegeneration and this was demonstrated by FJB-bright neuronal bodies at the site of PLP loss in AcPb-null brains. The physical injury of the needle also induced some FJB-positive neurons near the injection tract in both saline- and LPS-treated groups of all mice, however, FJB-positive neurons were found far from the injection site only in the brains of all AcPb-deficient mice challenged with LPS and none of the wild type or AcP-deficient mice. Interestingly, the LPS-induced neuronal loss in AcPb mice was not yet detectable at 24 hours (*not shown*) suggesting it was not an immediate consequence of LPS administration. These results indicate that AcPb can play an important role in neuro-

protection during and acute inflammatory response in the CNS, possibly by regulating the activity of IL-1.

DISCUSSION

We report here the identification of a novel splice variant of the IL-1 receptor family member IL-1R AcP, which we call AcPb. Due to conserved structural features and the tissue-specific regulation of expression, we believe this transcript to be more than simply a splicing anomaly. The new form is identical to the classic form of AcP in its extracellular and transmembrane domains and in the membrane-proximal portion of the cytoplasmic domain. The C-terminal portion of the cytoplasmic domain differs from that of classic AcP in two ways. First, although it retains motifs and predicted structure shared among all TIR domains, its overall sequence differs from that of classic AcP. Second, it has an extra approximately 140 amino acids to the C-terminal side of the TIR domain. AcPb is expression is largely restricted to the central nervous system. We speculated initially that this novel form would diversify IL-1 signaling in the CNS, but to our surprise, we found instead that it negatively regulates the expression of a subset of IL-1 induced genes and thus may serve to limit the inflammatory effects of IL-1 in the CNS.

IL-1 and the IL-1 receptors are expressed in the brain and IL-1 is known to regulate a number of adaptive physiologic processes in the CNS, including sickness behavior (Konsman et al., 2002), fever response **(Dinarello, 2004)** and activation of the pituitary-adrenal axis (Besedovsky et al., 1986) . Many of these activities are thought to result from direct effects of IL-1 on neuronal cells. Although IL-1 is an inflammatory cytokine, its expression is usually low in the brain and it is not itself toxic to neurons when administered acutely into the healthy brain. It is clear, however, that cellular responses to IL-1 are modulated by the physiologic state and under various pathological conditions IL-1 has been shown to exacerbate neurodegeneration, for example, in response to traumatic brain injury, seizure or acute ischemic insult (reviewed by (Bartfai et al., 2007; Rothwell et al., 1997). Unregulated IL-1 activity has also been implicated in mental retardation associated with multisystem inflammatory disease (Goldbach-Mansky et al., 2006). The mechanisms by which IL-1 influences these centrally-mediated effects are **likely to be** complex and may involve, in part, neuronal-specific signaling (Davis et al., 2006; Pizzi et al., 2002; Srinivasan et al., 2004; Tsakiri et al., 2008). The existence and structure of the AcPb molecule suggests that it could play a role in determining specific IL-1-dependent outcomes in the CNS.

The identity of the extracellular and transmembrane portions of AcP and AcPb indicates that AcPb should be recruited to ligand-bound IL-1 receptor in similar fashion to AcP, and indeed, we have demonstrated that this is the case (**Figure 3**). We presume that AcPb can also be recruited to other AcP-utilizing receptors, such as ST2 (Ali et al., 2007; Chackerian et al., 2007; Palmer et al., 2008) and IL-1Rrp2 (Towne et al., 2004), once they have bound their ligands. IL-1Rrp2 was initially cloned from brain (Lovenberg et al., 1996) and ST2 mRNA is found in the CNS (*unpublished observations* and (Andre et al., 2005)), so the functions of these two receptors and their ligands IL-33 and the IL-1F proteins may also be modified by AcPb. Despite the ability to form a trimolecular complex with IL-1 and IL-1 receptor, AcPb does not permit the recruitment of key signaling molecules utilized by TIR

domain-containing receptors to mediate inflammation. Neither MyD88 nor IRAK-4 is able to bind to the AcPb-containing complex. Furthermore, IL-1 signaling via the IL-1R/AcPb complex does not lead to phosphorylation of MAP kinases including p38, JNK and Erk. We have observed the same general inability to induce canonical signaling responses whether either IL-1α or IL-1β is used, and also when AcPb is co-expressed with chimeric receptors containing the cytoplasmic domains of other IL-1R family members, including ST2 and IL-1Rrp2 (*unpublished data and* (Born et al., 2000)). Thus, the signaling function, if any, of AcPb is considerably different from that of AcP. We confirmed this by demonstrating that IL-1 was not able to induce IL-2, IL-5 and IL-6 in EL4 cells expressing IL-1R and AcPb. It is likely that the inability to recruit key signaling components to the receptor and promote cytokine induction is due to the changed configuration in the DD loop and αD helix regions of the AcPb TIR domain and to the altered charge distribution pattern on its surface, both of which could affect interaction with other proteins. It is interesting to note that SIGIRR, another TIR domain-containing transmembrane protein postulated to play a negative role in IL-1 and TLR signaling (Garlanda et al., 2007; Qin et al., 2005; Thomassen et al., 1999; Wald et al., 2003), also has several prolines in the same region as those which disrupt the αD helix in AcPb.

Because EL4 is a lymphocyte line and AcPb is expressed only in CNS tissues and perhaps only in neurons, it was possible that key signaling intermediates required for AcPb function were missing from EL4 cells. Thus, we tested the ability of AcPb to transduce IL-1 responses in primary cortical neurons. In contrast to AcP, introduction of AcPb into neuronal cultures derived from mice deficient in all splice forms of AcP led to only a low level induction of a limited set of genes, of perhaps questionable significance. This result indicated that even if AcPb interacts with novel co-factors or utilizes distinct signal transduction pathways it is still unable to mediate a robust IL-1 response at the level of gene induction. Because the pattern of in situ hybridization suggested that AcPb was likely expressed in cells which also express AcP, we co-introduced both genes into AcP-deficient neurons. In this setting, genes induced by IL-1 fell into one of two categories. Some genes (e.g., GBP2, CCL2 and CXCL2) were induced as strongly in co-expressing cells as in cells expressing only AcP. Expression of other genes (e.g. ATF3, ICAM-1 and C/EBP delta), however, was dramatically inhibited when AcPb was co-expressed with AcP. Thus, consistent with its retention of a variant TIR domain, AcPb is not a general inhibitor of IL-1 function, but rather changes the quality of the IL-1 response by skewing the gene expression pattern.

We utilized AcPb-specific exon 12 knockout animals along with AcP-deficient mice to examine the relative in vivo contribution of AcP and AcPb to peripherally-induced versus locally-induced inflammation in the CNS. It was previously reported that IL-1R-deficiency protects mice from Th17-mediated inflammation and CNS damage in a model of EAE (Sutton et al., 2006). Consistent with these findings, we observed a profound protective effect of AcP deficiency in EAE however the loss of AcPb conferred no such protection compared to wild type controls. In an acute model of local LPS challenge in the CNS, however, the absence of AcPb expression led to neuronal loss in response to an otherwise non-toxic innate immune stimulation. This in vivo result indicated that, possibly by

modulating the intracellular signaling and gene expression response to LPS-induced IL-1, AcPb expression may buffer the neurotoxic effects of IL-1 or possibly the other AcP-utilizing cytokines. Interestingly, the transcription factor ATF3, one of the IL-1-induced genes whose induction was dramatically reduced by AcPb co-expression in our neuronal culture, has been implicated in mediating neurodegeneration in various experimental settings (Chen et al., 2008; Song et al., 2008). In light of this finding, it will be interesting to further investigate how different environmental and pathologic conditions modulate the relative expression of AcP and AcPb. The ratio of AcP and AcPb expression at the cellular level could determine the neuronal outcome in settings that involve excess IL-1 activity.

What is the mechanism by which AcPb has a selective inhibitory effect on IL-1 induced gene expression? One hypothesis would be that AcPb generally inhibits all IL-1 responses in an AcP-competitive manner through a failure to recruit MyD88 and IRAK4, and that the effect on expression of particular genes is determined by the overall strength of signal required for induction of each gene. Such a phenomenon has been reported in the form of different thresholds of Erk-dependent activation of IL-1 and TNF genes (Papoutsopoulou et al., 2006). We tried to address this by looking at induction of individual genes as a function of IL-1 dose in 3T3 mouse fibroblasts expressing AcP alone or AcP + AcPb. We saw no shift in the dose-response curve for any gene when AcPb was present (*unpublished*). Therefore, we have no evidence to support the "strength-of-signal" hypothesis. Another hypothesis would be that AcPb initiates a novel signaling function that is insufficient for gene induction on its own, but might be required for full induction of some genes and could involve association with novel adaptor proteins. Interestingly, novel forms of both MyD88 and IRAK have been identified that are primarily expressed in the brain (Kim et al., 2007; Su et al., 2007). Alternatively, the function could interfere with signals necessary for expression of other genes, for example by counteracting the ability of p38 to stabilize mRNAs. Yet another hypothesis postulates that the functional IL-1 receptor complex contains not just a single molecule each of IL-1R and AcP, but several. In this case, a mixture of IL1R/AcP and IL1R/AcPb heterodimers would not recruit the full complement of MyD88 and IRAK-4, and perhaps other molecules, as compared to a receptor complex without AcPb. Little is known about the multimeric state of the IL-1R complex, although there is some evidence that higher-order aggregates are required for IL-1 signaling (Guo et al., 1995).

In addition to its altered TIR domain, AcPb differs from AcP in that it contains a C-terminal "tail" of approximately 140 amino acids. C-terminal tails are also found in the IL-1R family members SIGIRR, TIGIRR and APL, although none are homologous to the AcPb sequence. It is interesting that none of these C-terminal tail-containing receptors, although they contain TIR domains, is capable of activating standard IL-1 signaling pathways when artificially brought into proximity with either IL-1R or AcP (Born et al., 2000). Although this has obvious implications for regulation of signaling, we have found that the presence or absence of the C-terminal tail does not affect the inability of AcPb to mediate IL-1/IL-1R signaling (*unpublished*). The C-terminal tail could of course mediate a function entirely independent of IL-1 signaling. In the case of the X-linked receptor family member APL, which is genetically associated with cognitive function and autism in humans, the C-terminal

extension is reported to interact with neuronal calcium sensor-1 and regulate neuron growth (Bhat et al., 2008; Gambino et al., 2007; Gao et al., 2008; Piton et al., 2008; Tabolacci et al., 2006). The C-terminal extension of AcPb also offers the opportunity to interact with other proteins, recruiting them to the receptor complex or perhaps affecting the cellular location of the complex.

The findings in this manuscript extend the range of regulatory mechanisms used to control IL-1 activity. In addition to the blockade of the type I IL-1 receptor by IL-1ra, and the decoy function for IL-1β of either membrane-bound or soluble type 2 IL-1R, there are now three regulatory complexes involving the Accessory Protein. Soluble AcP greatly enhances the ability of soluble type 2 IL-1R to inhibit IL-1 action (Smith et al., 2003). On the cell membrane, full-length type 2 IL-1R bound to IL-1 can recruit full-length, classical AcP to the complex, and thereby decoys not only the ligand but also a key signaling receptor subunit away from productive interaction with IL-1 bound type 1 IL-1R (Lang et al., 1998; Malinowsky et al., 1998) There is also an inhibitory activity of soluble AcP alone; although the mechanism has not been biochemically defined, it has been attributed to interaction with the membrane complex of IL-1 bound to the type 1 IL-1R (Smeets et al., 2005). All of the above regulatory mechanisms act to dampen or eliminate global IL-1 responses. The novel regulatory mechanism described in this paper differs in that only certain IL-1 responses are inhibited. Thus, rather than eliminating an IL-1 signal entirely, the quality of the signal is altered. We are not aware of similar findings having previously been reported.

Another paper has recently been published describing this same splice variant of AcP (Lu et al., 2008) The authors of that study reach conclusions about its function which differ from ours. We do not know how to explain the discrepancy except that their conclusions were drawn predominantly from over-expression studies in HEK293 cells.

EXPERIMENTAL PROCEDURES

cDNA cloning

A computational search for novel sequences with similarity to members of the IL-1R family was applied to human genomic DNA sequence (Celera human genome assembly R23-sequence CRA27000022534528). An open reading frame was identified on chromosome 3q28 that was 31% identical to exon 12 of IL-1RAcP. 5' RACE and PCR were used to clone full length AcPb sequence from human cDNA libraries. An orthologous AcPb exon 12 was identified in mouse genomic sequence that is 92.4 % identical to the human exon at the amino acid level and full-length AcPb cDNA was cloned from mouse total brain.

PCR

First strand cDNA from multiple human and mouse tissues was amplified by real-time PCR using Taqman® primer and probe sets specific for AcP or AcPb. The sequences of the primers and probes are as follows (5' to 3'). Human AcP: primer 1 (GGGCAGGTTCTGGAAGCA) at 900 nM , primer 2 (GCTAGACCGCCTGGGACTTT) at 900 nM , and FAM probe (TCACTGGCATGGCCACCTGCAG) at 200 nM. Human AcPb: primer 1 (TCCAAGCACCGAGGGAAGT) at 900 nM , primer 2

(AGGTGATTCTCTCCTTCACAGTAGGT) at 900 nM , and FAM probe (CCGCCACCTGCCGCTGTTG) at 200 nM. Mouse AcP: primer 1 (GGGCAACATCAACGTCATTTT) at 300 nM, primer 2 (CAGCTCTTTCACCTTCATGTCCTT) at 50 nM, and FAM probe (CACAGCTTTGTACTGCACT) at 200 nM. Mouse AcPb: primer 1(GGAGTTTAAGCTGGGTGTCATGT) at 50 nM, primer 2 (TGCTCAAGCGGACGGTACT) at 50 nM, and FAM probe (CCATTGCCACTAAGC) at 200 nM. All reactions were run in triplicate and Ct (threshold) values to determine relative expression were normalized against the housekeeper gene HPRT. cDNAs from pooled human brain regions were obtained from Clontech. Real-time PCR profiling of spinal cord tissue from mice with EAE was performed using a custom Taqman® Low density Array (Applied Biosystems). For RTPCR analysis of AcP and AcPb expression in cultured cells, day 16 embryonic mouse hippocampal neurons and astrocytes were cultured as previously described (Srinivasan et al, 2004). Total RNA was isolated with trizol reagent (Invitrogen) as recommended by the manufacturer and 1 microgram of reverse-transcribed cDNA was amplified for 35 cycles using the following primers: AcP (mAcP.cyto.foward 5'-TGTTTCCTATGCAAGAAATGTGGAAGAAGAGG-3', mAcP.cyto.rev: 5'-TGCTTGTCATTGCTAGACCACCTGG-3') and AcPb (mAcP.cyto.foward: 5'-TGTTTCCTATGCAAGAAATGTGGAAGAAGAGG-3', mAcPb.1.rev: 5'-ATGGGGTTGCTCAAGCGACGGTACTCCAC-3'). PCR products were resolved on a 1% agarose gel and stained with ethidium bromide.

In situ hybridization

Antisense ^{35}S UTP riboprobes specific for mouse AcP or AcPb mRNAs were made using RNA polymerase reactions with linearized plasmids containing either mouse AcP exon 12 or AcPb exon 12. Adult mouse brain sections were hybridized and exposed to radiographic emulsion for 5 or 12 days. As a control, sense strand riboprobe hybridizations were performed. Sections were stained with hematoxylin and eosin for bright field images.

Computational modeling of TIR domains

The models of AcP and AcPb TIR domains were built based on alignments to the crystal structure of the Toll/Interleukin-1 receptor (TIR) domain of human IL-1RAPL (Khan et al., 2004), PDB id 1T3G, chain A. The protein structure models were built using the Homology Modeling method within the Molecular Operating Environment (MOE, Chemical Computing Group, Montreal, Quebec, Canada).

EL4 stable lines

EL4.16a cells (IL-1R^{+}/AcP[-] mouse lymphoma line) were transduced with retroviral vectors (Amgen, Inc.) encoding full-length muAcP or muAcPb and selected by FACS sorting for positive surface expression of the AcP extracellular domain with M215 antibody (rat IgG, Amgen Inc.). For immunoprecipitation experiments, 3×10^7 cells were incubated with or without IL-1β (100 ng/mL) at 37°C for 3 minutes. Whole cell lysates were immunoprecipitated with the M215 antibody then subjected to SDS-PAGE. Co-precipitation of IL-1R or signaling molecules was evaluated by Western blotting with anti-muIL-1R, anti-MyD88 or anti-IRAK4 polyclonal antibodies (P2, Amgen Inc., Chemicon # 16527 or

#16529 and Cell Signaling Technologies #4363, respectively). For IL-2, IL-5 and IL-6 measurements, 0.25×10^6 cells were incubated in triplicate for 24 hours in the presence of 300 ng/mL ionomycin and 100 pg/mL PMA (both from Sigma) plus or minus IL-1β (100 pg/mL). Cytokine levels in the supernatants were quantified by Luminex-based multiplex assay (Luminex Corp.) using reagents from Biosource International. To measure induction of phosphorylated kinases, 2.0×10^7 cells were incubated with or without IL-1β (10 ng/mL) or 0.5M sorbitol at 37°C for various lengths of time and then immediately lysed. Equivalent amounts of lysates (approximately 0.4×10^6 cell equivalents/lane) were subjected to SDS-PAGE and Western blotting was performed with phospho-specific antibodies phospho-p44/p42 (Cell Signaling Technologies #9101), phospho-JNK (Cell Signaling Technologies #9251), and phosphop38 (Cell Signaling Technologies #9211).

Animals used and description of AcPb knockout mice

Homozygous AcP-deficient mice (B6;129S-*Il1rap)* were obtained from Taconic Laboratories and were completely backcrossed onto a C57BL/6Tac background, as confirmed by microsatellite analysis (performed by Charles River Laboratories). AcPb knockout mice (B6;129-*IL1racpb*) were generated utilizing a 10.6 kb targeting cassette that replaced the entire AcPb-specific exon 12 with a neomycin resistance gene (as shown in Figure 1). The upstream exon 12 of classic AcP and the intervening 7.3 kb intron were left intact in order to maintain expression of normal full length AcP. 129 embryonic stem (ES) cells were transfected with the targeting vector and selected under standard conditions. ES cell clones were transplanted into female Black-Swiss females and homozygous animals were backcrossed completely onto a C57BL/6Tac background, as confirmed by microsatellite analysis (performed by Charles River Laboratories). *IL1racpb* mice bred normally and appeared phenotypically normal. Wild type and knockout mice were subsequently obtained from Taconic Labs, where they were maintained under standard germ-free barrier conditions. All animal studies were reviewed and approved by the Amgen Animal Care and Use Committee or were conducted according to the Canadian Council on Animal Care guidelines, as administered by the Laval University Animal Welfare Committee.

Cortical neuron cultures

Pregnant mice (E17-E18) were anesthetized by CO_2 and brains were surgically removed. Micro-dissected cortical tissue was digested for 45 minutes at 37°C in papain solution (Worthington Biochemical) then gently disassociated in DMEM + 10% FBS with a 10 mL pipette followed by gentle filtration through a 40 μm cell strainer. Single cell suspensions were plated into 6 well tissue culture dishes pre-coated with 0.1 mg/ml Poly-L-Ornithine (Sigma) and placed in a 37 °C incubator with 5% CO_2 (approximately 1×10^6 cells/well). 30 minutes later, the medium was replaced with serum-free neuronal growth medium (2% B-27 supplement + 1% PSG in Neurobasal Medium (Invitrogen Corp)) and cultures were maintained for nine days to allow for neuronal maturation. For immunostaining, cells were fixed for 15 minutes with 2% paraformaldehyde then permeabilized with 0.1% Triton. Cells were blocked with SuperBlock (Pierce) and 2.5% normal horse serum (Hyclone) for 1.5 hours then incubated with primary antibodies diluted in TBS + 1% horse serum + 0.05% Tween-20. For neuronal staining: anti-MAP-2 (Chemicon Ab5622), for glial cell staining:

anti-GFAP (Chemicon MAB3402). Staining was completed using NovRed substrate and reagents from the Vectastain ABC peroxidase system (Vector Laboratories). AcP or AcPb expression and induction of CCL2 mRNA was determined by RT-PCR analysis of total RNA.

Microarray analysis

Cortical neuron cultures were established from homozygous AcP-deficient mice (B6;129S-*Il1rap*) (Cullinan et al., 1998) as described above. After 7 days of culture, cells were transduced at an MOI of 5 with lentivirus vector (pLV401, Amgen Inc.) engineered to express either a cytoplasmic domain-truncated form of IL-2Rα (CD25, control) or full length muAcP or muAcPb. Following incubation for 2 hours at 37° C, cells were washed with PBS and placed back in Neurobasal growth medium and cultured for 2 days. On day 9, cells were left untreated or stimulated in triplicate with IL-1β (10 ng/mL) for either 4 or 16 hours and then collected for total RNA preparation. Receptor expression and CCL2 induction was confirmed by RT-PCR and for microarray analysis, individual biological replicate RNAs were separately labeled and hybridized to Affymetrix Mo430 microarray chips containing approximately 45,000 probe sets (Affymetrix). Data from individual arrays were first normalized then compared as ratios between sample sets at the level of the reporter probes, generating an error-weighted gene expression ratio using the Resolver software system (Rosetta Biosoftware). Sequences with high noise between replicate experiments were filtered out, and expression changes were calculated using the Resolver "Affymetrix with Reporters" error model. Relative error was calculated in logarithmic space, and converted to a mean error in Fold-Change.

Characterization of knockout mice

To examine the expression of AcP and AcPb in knockout mice, whole brains were isolated from wild type, AcP$^{-/-}$ and AcPb$^{-/-}$ animals and total RNA was evaluated by RTPCR amplification of AcP, AcPb and the control gene HPRT. Phenotypic analysis of age-matched brains was assessed by Weil and Thionine staining to reveal cell bodies and myelin, respectively (Neuroscience Associates, Knoxville, TN). Briefly, brains were perfused, embedded and sectioned at 35μm in the coronal plane through the entire brain. Staining was evaluated at 840μm intervals. To measure the responsiveness of peripheral cells to IL-1β, spleens were harvested from individual C57Bl/6, AcP$^{-/-}$, and AcPb$^{-/-}$ mice (n=3/group) and RBC-free single cell cultures were established. Cells were left untreated or stimulated with hIL-1β (at 0.43, 4.3 or 43 ng/ml) or LPS (86ng/ml). Supernatants were collected 48 hours later and the concentration of IL-6 produced was determined by ELISA (R&D Systems). To examine expression of AcP protein isoforms in total brain, protein lysates were generated by homogenization of brain tissue in TPER lysis buffer (Pierce) using a TissueLyzer system (Qiagen). Cleared lysates were immunoprecipitated at 4°C with anti-muAcP (M215) and proteins were subjected to SDS-PAGE, transferred to nitrocellulose membranes and incubated overnight with a rabbit polyclonal antibody against muAcP that detects both AcP and AcPb (P2, Amgen Inc.). Similar M215 immunoprecipitations of AcP and AcPb from stable EL4 cell lines (described above) were included as controls on the gel. Briefly, lysates were generated from 100 million cells in 3.2 ml of lysis buffer and AcP and AcPb were immunoprecipitated from 1 ml of lysate during an overnight incubation at 4°C

with the M215 Ab, as above. Immunoprecipitated proteins, corresponding to approximately 6 million cell equivalents, were analyzed by Western blot alongside the brain immunoprecipitations.

EAE

To induce EAE, 10 week old female C57Bl/6 (n=15), AcP$^{-/-}$ (n=18) and AcPb$^{-/-}$ (n=14) mice were immunized s.c. with 150 μg myelin oligodendrocyte glycoprotein amino acids 35-55 (MOG$_{35-55}$; Amgen Inc., Seattle, WA) in an emulsion with CFA (Sigma, St. Louis, MO) containing 400 μg *M. tuberculosis* H37 Ra (Difco Lawrence, KS) on day 0. Pertussis toxin (350 ng/mouse) in PBS was injected i.v. 48 hr after immunization. Animals were monitored, weighed, and scored for clinical disease every other day until disease was observed then daily thereafter. Disease onset was defined as a score of 1 or more for more than two successive days. EAE scoring was performed as follows: 0, no abnormality; 1, a limp tail; 2, impairment of righting reflex or abnormal gait; 3, severe hind limb weakness, partial hind limb paralysis; 4, complete hind limb paralysis, mobile using forelimbs. Mice were euthanized on day 20 post-immunization. Spinal cords from 5 naïve mice and 5 immunized mice per group were harvested for Real Time PCR low density array analysis. GraphPad Prism 5.0 (GraphPad software Inc.) was used to determine statistical significance.

Intracerebral LPS injection and histology

Wild type, AcP$^{-/-}$ and AcPb$^{-/-}$ mice (approximately 10-weeks old) were acclimated to standard laboratory conditions at Laval University (14 hours light, 10 hours dark cycle) with free access to rodent chow and water. Isofluorane was used to anesthetize the mice and the site for LPS injection was stereotaxically determined by microscopy. To reach the injection site, the coordinates from the bregma were -2 mm lateral and -3 mm dorsoventral. One μl of 0.9% NaCl solution or LPS (1.0 mg/ml) was injected for a period of 1 minute using a micro-injection pump (Razel Scientific Instruments, Stanford, CT). One, 3 and 7 days later, mice were deeply anesthetized by i.p injection of a ketamine hydrochloride (91 mg/ml) and xylazine (9.1 mg/ml) solution. They were quickly transcardially perfused with a 0.9% saline solution followed by 4% paraformaldehyde/3.8% Borax solution, pH 9 at 4 °C. Immediately after fixation, brains were removed from the skulls and post-fixed in 4% paraformaldehyde/ 3.8% Borax solution, pH 9 for 24 hours. Following post-fixation, brains were placed overnight in a solution of 4% paraformaldehyde/3.8% Borax solution, pH 9 containing 10 % sucrose. The brains were mounted on a microtome (Reichert-Jung, Cambridge Instruments Company, Deerfield, IL, USA), frozen with dry ice and sliced into 25 μm coronal sections from olfactory bulb to the end of the medulla. The obtained slices were placed in a cold cryoprotectant solution (0.5 M sodium phosphate buffer pH 7.3, 30 % ethylene glycol, 20 % glycerol) and stored at −20 °C. IL-1β and Proteolipid protein (PLP) mRNA expression was detected via *in situ* hybridization (ISH) as previously described (Laflamme et al., 1999) and neuronal cell death was characterized by Fluoro-Jade B (FJB) method (Nadeau and Rivest, 2003).

Supplementary Material

Refer to Web version on PubMed Central for supplementary material.

Acknowledgments

References

Ali S, Huber M, Kollewe C, Bischoff SC, Falk W, Martin MU. IL-1 receptor accessory protein is essential for IL-33-induced activation of T lymphocytes and mast cells. Proc Natl Acad Sci U S A. 2007; 104:18660–18665. [PubMed: 18003919]

Alpert D, Schwenger P, Han J, Vilcek J. Cell stress and MKK6b-mediated p38 MAP kinase activation inhibit tumor necrosis factor-induced IkappaB phosphorylation and NF-kappaB activation. J Biol Chem. 1999; 274:22176–22183. [PubMed: 10428782]

Andre R, Lerouet D, Kimber I, Pinteaux E, Rothwell NJ. Regulation of expression of the novel IL-1 receptor family members in the mouse brain. J Neurochem. 2005; 95:324–330. [PubMed: 16086690]

Bartfai T, Sanchez-Alavez M, Andell-Jonsson S, Schultzberg M, Vezzani A, Danielsson E, Conti B. Interleukin-1 system in CNS stress: seizures, fever, and neurotrauma. Ann N Y Acad Sci. 2007; 1113:173–177. [PubMed: 17656565]

Besedovsky H, del Rey A, Sorkin E, Dinarello CA. Immunoregulatory feedback between interleukin-1 and glucocorticoid hormones. Science. 1986; 233:652–654. [PubMed: 3014662]

Bhat SS, Ladd S, Grass F, Spence JE, Brasington CK, Simensen RJ, Schwartz CE, Dupont BR, Stevenson RE, Srivastava AK. Disruption of the IL1RAPL1 gene associated with a pericentromeric inversion of the X chromosome in a patient with mental retardation and autism. Clin Genet. 2008; 73:94–96. [PubMed: 18005360]

Blomer U, Naldini L, Kafri T, Trono D, Verma IM, Gage FH. Highly efficient and sustained gene transfer in adult neurons with a lentivirus vector. J Virol. 1997; 71:6641–6649. [PubMed: 9261386]

Born TL, Smith DE, Garka KE, Renshaw BR, Bertles JS, Sims JE. Identification and characterization of two members of a novel class of the interleukin-1 receptor (IL-1R) family. Delineation Of a new class of IL-1R-related proteins based on signaling. J Biol Chem. 2000; 275:41528. [PubMed: 11134060]

Burns K, Janssens S, Brissoni B, Olivos N, Beyaert R, Tschopp J. Inhibition of interleukin 1 receptor/ Toll-like receptor signaling through the alternatively spliced, short form of MyD88 is due to its failure to recruit IRAK-4. J Exp Med. 2003; 197:263–268. [PubMed: 12538665]

Chackerian AA, Oldham ER, Murphy EE, Schmitz J, Pflanz S, Kastelein RA. IL-1 receptor accessory protein and ST2 comprise the IL-33 receptor complex. J Immunol. 2007; 179:2551–2555. [PubMed: 17675517]

Chen HM, Wang L, D'Mello SR. Inhibition of ATF-3 expression by B-Raf mediates the neuroprotective action of GW5074. J Neurochem. 2008; 105:1300–1312. [PubMed: 18194435]

Cullinan EB, Kwee L, Nunes P, Shuster DJ, Ju G, McIntyre KW, Chizzonite RA, Labow MA. IL-1 receptor accessory protein is an essential component of the IL-1 receptor. J Immunol. 1998; 161:5614–5620. [PubMed: 9820540]

Davis CN, Mann E, Behrens MM, Gaidarova S, Rebek M, Rebek J Jr. Bartfai T. MyD88-dependent and -independent signaling by IL-1 in neurons probed by bifunctional Toll/IL-1 receptor domain/BB-loop mimetics. Proc Natl Acad Sci U S A. 2006; 103:2953–2958. [PubMed: 16477040]

Dinarello CA. Infection, fever, and exogenous and endogenous pyrogens: some concepts have changed. J Endotoxin Res. 2004; 10:201–222. [PubMed: 15373964]

Gambino F, Pavlowsky A, Begle A, Dupont JL, Bahi N, Courjaret R, Gardette R, Hadjkacem H, Skala H, Poulain B, et al. IL1-receptor accessory protein-like 1 (IL1RAPL1), a protein involved in

cognitive functions, regulates N-type Ca2+-channel and neurite elongation. Proc Natl Acad Sci U S A. 2007; 104:9063–9068. [PubMed: 17502602]

Gao X, Xi G, Niu Y, Zhang S, Fu R, Zheng Z, Zhang K, Lv S, He H, Xue M, Zhang F. A study on the correlation between IL1RAPL1 and human cognitive ability. Neurosci Lett. 2008; 438:163–167. [PubMed: 18467032]

Garlanda C, Di Liberto D, Vecchi A, La Manna MP, Buracchi C, Caccamo N, Salerno A, Dieli F, Mantovani A. Damping excessive inflammation and tissue damage in Mycobacterium tuberculosis infection by Toll IL-1 receptor 8/single Ig IL-1-related receptor, a negative regulator of IL-1/TLR signaling. J Immunol. 2007; 179:3119–3125. [PubMed: 17709526]

Goldbach-Mansky R, Dailey NJ, Canna SW, Gelabert A, Jones J, Rubin BI, Kim HJ, Brewer C, Zalewski C, Wiggs E, et al. Neonatal-onset multisystem inflammatory disease responsive to interleukin-1beta inhibition. N Engl J Med. 2006; 355:581–592. [PubMed: 16899778]

Guo C, Dower SK, Holowka D, Baird B. Fluorescence resonance energy transfer reveals interleukin (IL)-1-dependent aggregation of IL-1 type I receptors that correlates with receptor activation. J Biol Chem. 1995; 270:27562–27568. [PubMed: 7499217]

Huang J, Gao X, Li S, Cao Z. Recruitment of IRAK to the interleukin 1 receptor complex requires interleukin 1 receptor accessory protein. Proc Natl Acad Sci U S A. 1997; 94:12829–12832. [PubMed: 9371760]

Jiang Z, Johnson HJ, Nie H, Qin J, Bird TA, Li X. Pellino 1 is required for interleukin-1 (IL-1)-mediated signaling through its interaction with the IL-1 receptor-associated kinase 4 (IRAK4)-IRAK-tumor necrosis factor receptor-associated factor 6 (TRAF6) complex. J Biol Chem. 2003; 278:10952–10956. [PubMed: 12496252]

Khan JA, Brint EK, O'Neill LA, Tong L. Crystal structure of the Toll/interleukin-1 receptor domain of human IL-1RAPL. J Biol Chem. 2004; 279:31664–31670. [PubMed: 15123616]

Kim Y, Zhou P, Qian L, Chuang JZ, Lee J, Li C, Iadecola C, Nathan C, Ding A. MyD88-5 links mitochondria, microtubules, and JNK3 in neurons and regulates neuronal survival. J Exp Med. 2007; 204:2063–2074. [PubMed: 17724133]

Konsman JP, Parnet P, Dantzer R. Cytokine-induced sickness behaviour: mechanisms and implications. Trends Neurosci. 2002; 25:154–159. [PubMed: 11852148]

Laflamme N, Lacroix S, Rivest S. An essential role of interleukin-1beta in mediating NF-kappaB activity and COX-2 transcription in cells of the blood-brain barrier in response to a systemic and localized inflammation but not during endotoxemia. J Neurosci. 1999; 19:10923–10930. [PubMed: 10594073]

Lang D, Knop J, Wesche H, Raffetseder U, Kurrle R, Boraschi D, Martin MU. The type II IL-1 receptor interacts with the IL-1 receptor accessory protein: a novel mechanism of regulation of IL-1 responsiveness. J Immunol. 1998; 161:6871–6877. [PubMed: 9862719]

Li C, Zienkiewicz J, Hawiger J. Interactive sites in the MyD88 Toll/interleukin (IL) 1 receptor domain responsible for coupling to the IL1beta signaling pathway. J Biol Chem. 2005; 280:26152–26159. [PubMed: 15849357]

Lovenberg TW, Crowe PD, Liu C, Chalmers DT, Liu XJ, Liaw C, Clevenger W, Oltersdorf T, De Souza EB, Maki RA. Cloning of a cDNA encoding a novel interleukin-1 receptor related protein (IL 1R-rp2). J Neuroimmunol. 1996; 70:113–122. [PubMed: 8898719]

Lu HL, Yang CY, Chen HC, Hung CS, Chiang YC, Ting LP. A novel alternatively spliced interleukin-1 receptor accessory protein mIL-1RAcP687. Mol Immunol. 2008; 45:1374–1384. [PubMed: 17949817]

Malinowsky D, Lundkvist J, Laye S, Bartfai T. Interleukin-1 receptor accessory protein interacts with the type II interleukin-1 receptor. FEBS Lett. 1998; 429:299–302. [PubMed: 9662436]

Nadeau S, Rivest S. Glucocorticoids play a fundamental role in protecting the brain during innate immune response. J Neurosci. 2003; 23:5536–5544. [PubMed: 12843254]

Palmer G, Lipsky BP, Smithgall MD, Meininger D, Siu S, Talabot-Ayer D, Gabay C, Smith DE. The IL-1 receptor accessory protein (AcP) is required for IL-33 signaling and soluble AcP enhances the ability of soluble ST2 to inhibit IL-33. Cytokine. 2008; 42:358–364. [PubMed: 18450470]

Papoutsopoulou S, Symons A, Tharmalingham T, Belich MP, Kaiser F, Kioussis D, O'Garra A, Tybulewicz V, Ley SC. ABIN-2 is required for optimal activation of Erk MAP kinase in innate immune responses. Nat Immunol. 2006; 7:606–615. [PubMed: 16633345]

Piton A, Michaud JL, Peng H, Aradhya S, Gauthier J, Mottron L, Champagne N, Lafreniere RG, Hamdan FF, Joober R, et al. Mutations in the calcium-related gene IL1RAPL1 are associated with autism. Hum Mol Genet. 2008

Pizzi M, Goffi F, Boroni F, Benarese M, Perkins SE, Liou HC, Spano P. Opposing roles for NF-kappa B/Rel factors p65 and c-Rel in the modulation of neuron survival elicited by glutamate and interleukin-1beta. J Biol Chem. 2002; 277:20717–20723. [PubMed: 11912207]

Qin J, Qian Y, Yao J, Grace C, Li X. SIGIRR inhibits interleukin-1 receptor- and toll-like receptor 4-mediated signaling through different mechanisms. J Biol Chem. 2005; 280:25233–25241. [PubMed: 15866876]

Radons J, Dove S, Neumann D, Altmann R, Botzki A, Martin MU, Falk W. The interleukin 1 (IL-1) receptor accessory protein Toll/IL-1 receptor domain: analysis of putative interaction sites in vitro mutagenesis and molecular modeling. J Biol Chem. 2003; 278:49145–49153. [PubMed: 13679373]

Rothwell N, Allan S, Toulmond S. The role of interleukin 1 in acute neurodegeneration and stroke: pathophysiological and therapeutic implications. J Clin Invest. 1997; 100:2648–2652. [PubMed: 9389726]

Sims JE. IL-1 and IL-18 receptors, and their extended family. Curr Opin Immunol. 2002; 14:117–122. [PubMed: 11790541]

Sims JE, Smith DE. Regulation of interleukin-1 activity is enhanced by cooperation between the interleukin-1 receptor type II and interleukin-1 receptor accessory protein. Eur Cytokine Netw. 2003; 14:77–81. [PubMed: 12957787]

Smeets RL, Joosten LA, Arntz OJ, Bennink MB, Takahashi N, Carlsen H, Martin MU, van den Berg WB, van de Loo FA. Soluble interleukin-1 receptor accessory protein ameliorates collagen-induced arthritis by a different mode of action from that of interleukin-1 receptor antagonist. Arthritis Rheum. 2005; 52:2202–2211. [PubMed: 15986350]

Smith DE, Hanna R, Della F, Moore H, Chen H, Farese AM, MacVittie TJ, Virca GD, Sims JE. The soluble form of IL-1 receptor accessory protein enhances the ability of soluble type II IL-1 receptor to inhibit IL-1 action. Immunity. 2003; 18:87–96. [PubMed: 12530978]

Song DY, Yang YC, Shin DH, Sugama S, Kim YS, Lee BH, Joh TH, Cho BP. Axotomy-induced dopaminergic neurodegeneration is accompanied with c-Jun phosphorylation and activation transcription factor 3 expression. Exp Neurol. 2008; 209:268–278. [PubMed: 18036593]

Srinivasan D, Yen JH, Joseph DJ, Friedman W. Cell type-specific interleukin-1beta signaling in the CNS. J Neurosci. 2004; 24:6482–6488. [PubMed: 15269258]

Su J, Richter K, Zhang C, Gu Q, Li L. Differential regulation of interleukin-1 receptor associated kinase 1 (IRAK1) splice variants. Mol Immunol. 2007; 44:900–905. [PubMed: 16690127]

Sutton C, Brereton C, Keogh B, Mills KH, Lavelle EC. A crucial role for interleukin (IL)-1 in the induction of IL-17-producing T cells that mediate autoimmune encephalomyelitis. J Exp Med. 2006; 203:1685–1691. [PubMed: 16818675]

Tabolacci E, Pomponi MG, Pietrobono R, Terracciano A, Chiurazzi P, Neri G. A truncating mutation in the IL1RAPL1 gene is responsible for X-linked mental retardation in the MRX21 family. Am J Med Genet A. 2006; 140:482–487. [PubMed: 16470793]

Thomassen E, Renshaw BR, Sims JE. Identification and characterization of SIGIRR, a molecule representing a novel subtype of the IL-1R superfamily. Cytokine. 1999; 11:389–399. [PubMed: 10346978]

Towne JE, Garka KE, Renshaw BR, Virca GD, Sims JE. Interleukin (IL)-1F6, IL-1F8, and IL-1F9 signal through IL-1Rrp2 and IL-1RAcP to activate the pathway leading to NF-kappaB and MAPKs. J Biol Chem. 2004; 279:13677–13688. [PubMed: 14734551]

Tsakiri N, Kimber I, Rothwell NJ, Pinteaux E. Interleukin-1-induced interleukin-6 synthesis is mediated by the neutral sphingomyelinase/Src kinase pathway in neurones. Br J Pharmacol. 2008; 153:775–783. [PubMed: 18059318]

Wald D, Qin J, Zhao Z, Qian Y, Naramura M, Tian L, Towne J, Sims JE, Stark GR, Li X. SIGIRR, a negative regulator of Toll-like receptor-interleukin 1 receptor signaling. Nat Immunol. 2003; 4:920–927. [PubMed: 12925853]

Wesche H, Henzel WJ, Shillinglaw W, Li S, Cao Z. MyD88: an adapter that recruits IRAK to the IL-1 receptor complex. Immunity. 1997a; 7:837–847. [PubMed: 9430229]

Wesche H, Korherr C, Kracht M, Falk W, Resch K, Martin MU. The interleukin-1 receptor accessory protein (IL-1RAcP) is essential for IL-1-induced activation of interleukin-1 receptor-associated kinase (IRAK) and stress-activated protein kinases (SAP kinases). J Biol Chem. 1997b; 272:7727–7731. [PubMed: 9065432]

Xu Y, Tao X, Shen B, Horng T, Medzhitov R, Manley JL, Tong L. Structural basis for signal transduction by the Toll/interleukin-1 receptor domains. Nature. 2000; 408:111–115. [PubMed: 11081518]
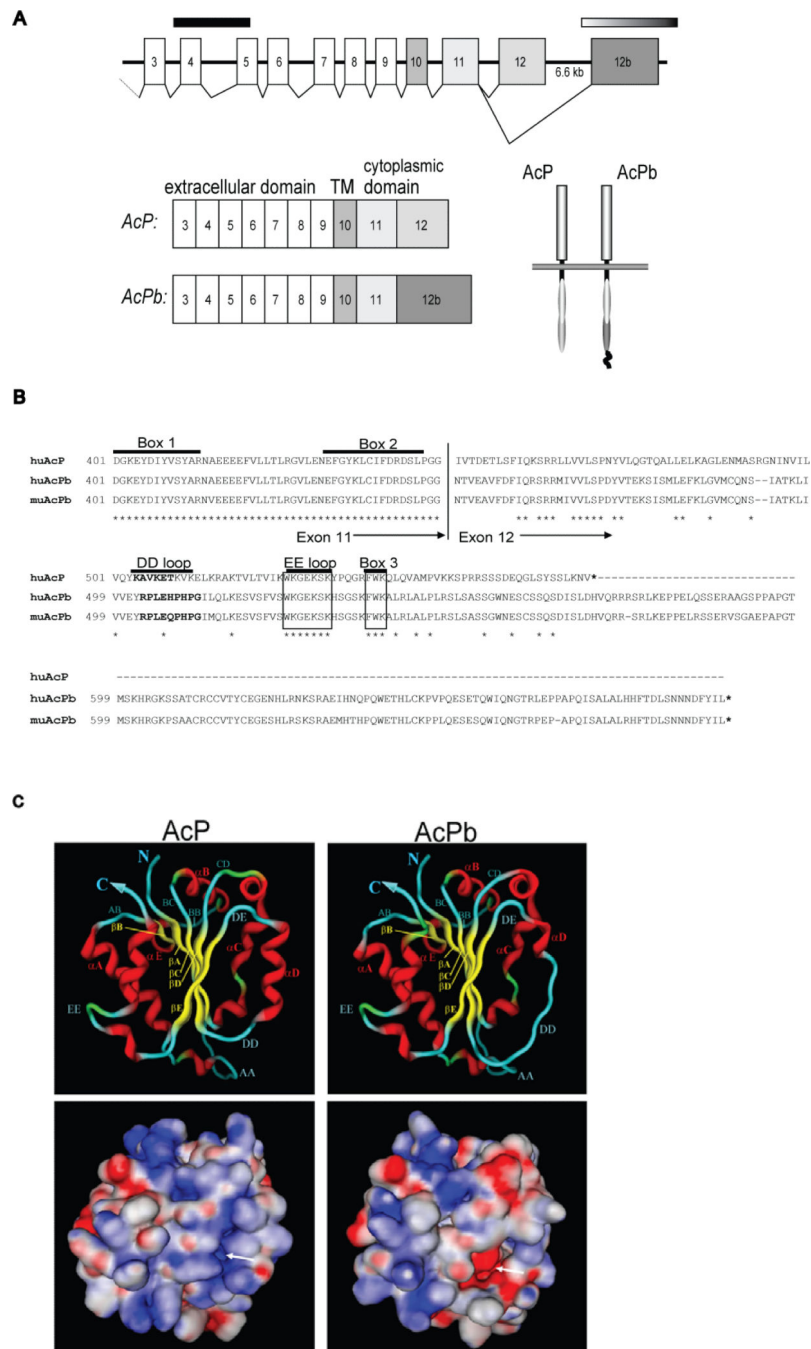
Figure 1. Genomic organization, sequence and TIR domain structural models of AcP isoforms
A, intron-exon map of human AcP locus and alternative splicing that leads to mRNA isoforms. Shown are the translated exons (3-12) that encode the mature AcP protein. The solid black bar indicates the extracellular exons that are deleted in the *il1rap* AcP knockout (Cullinan et al., 1998) and the faded bar indicates the specific exon 12b that is deleted in AcPb knockout animals (*described in text*). **B**, Alignment of the alternative C termini of AcP and AcPb isoforms. Stars indicate conserved residues between human AcP and human AcPb. Specific structural or signaling-associated motifs are indicated. **C**, Computational

models of AcP and AcPb TIR domains. Structural folds of the ribbon structure are labeled following the convention of (Khan et al., 2004). Beta sheets are indicated in yellow, alpha helices in red and loops in blue. Shown on the bottom is the identical view with predicted surface electrostatics. Full red is equivalent to -40 kcal/mol negative charge; full blue equivalent to 40 kcal/mol positive charge and white is neutral charge. The arrow indicates the region of significant charge difference caused by the disruption of the αD helix in AcPb.
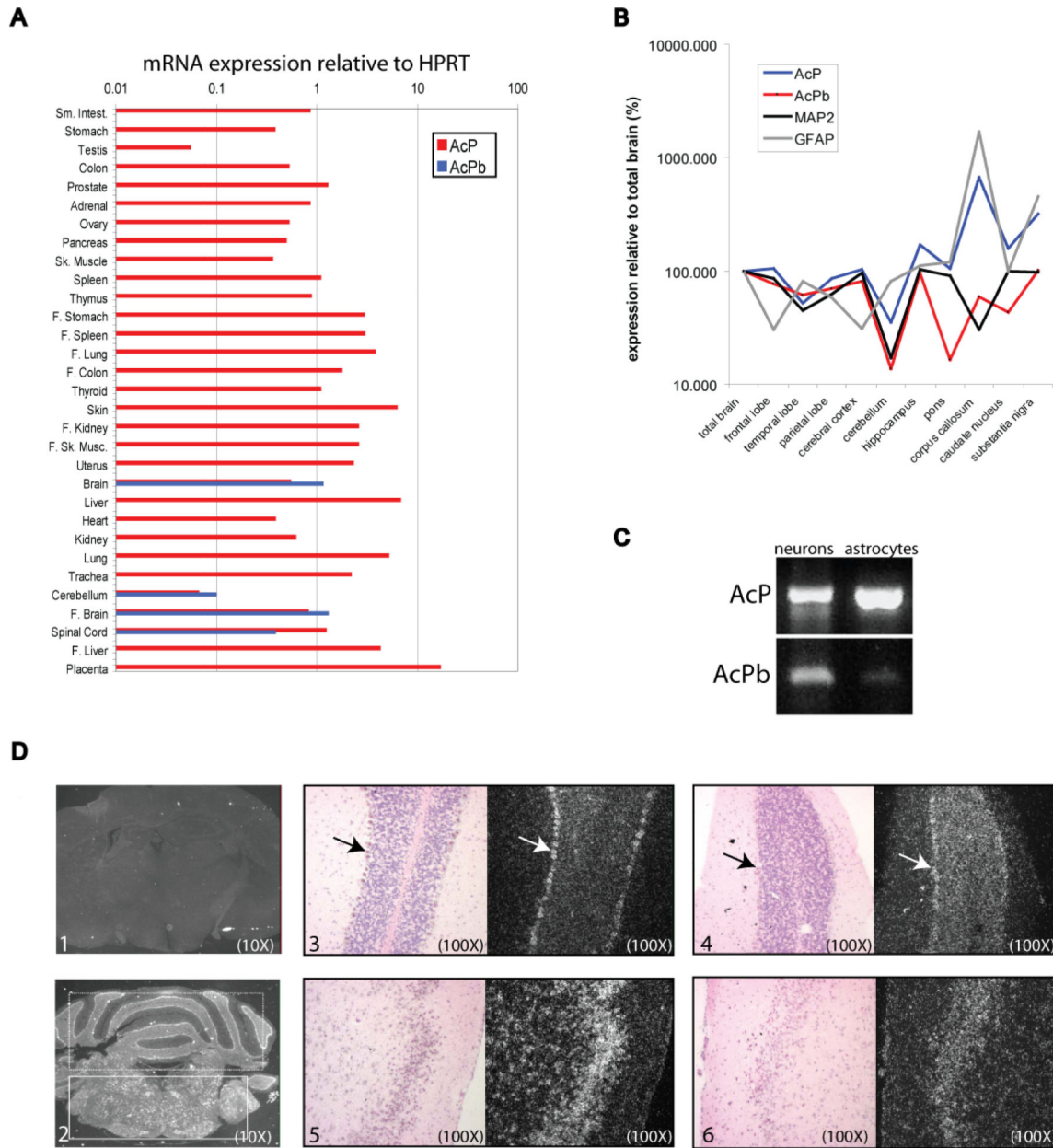
Figure 2. mRNA expression profile of AcP and AcPb

A, Relative mRNA level of AcP and AcPb isoforms in human tissues as determined by real time PCR and presented as expression relative to HPRT. Abbreviations: 'F', fetal, 'sm', small, 'sk', skeletal. **B**, Normalized relative expression of AcP and AcPb mRNAs across isolated human brain regions as compared to a neuronal- and astrocyte -specific gene (MAP2 and GFAP, respectively). Relative expression (to HPRT) for each gene in each region was normalized to its overall expression in total brain (set to 100%).C, RT-PCR amplification of AcP and AcPb mRNAs from primary hippocampal neuron and astrocyte cultures. D, In situ hybridization of adult mouse brain with RNA probes specific for AcP or AcPb isoforms. **1**, whole brain hybridized with sense strand control probe. **2**, whole brain hybridized with AcP antisense probe. Cerebellum is indicated with dashed box and the brain

stem with a solid box. **3**, **4**, Bright field and dark field images of cerebellum hybridized with either AcP (**3**) or AcPb (**4**) antisense probes. Positively hybridizing Purkinje cells are indicated with an arrow for both probe sets. **5**, **6**, Bright field and dark field images of forebrain hybridized with either AcP (**5**) or AcPb (**6**) antisense probes. Positively hybridizing neuronal cell bodies are visible with both probes.
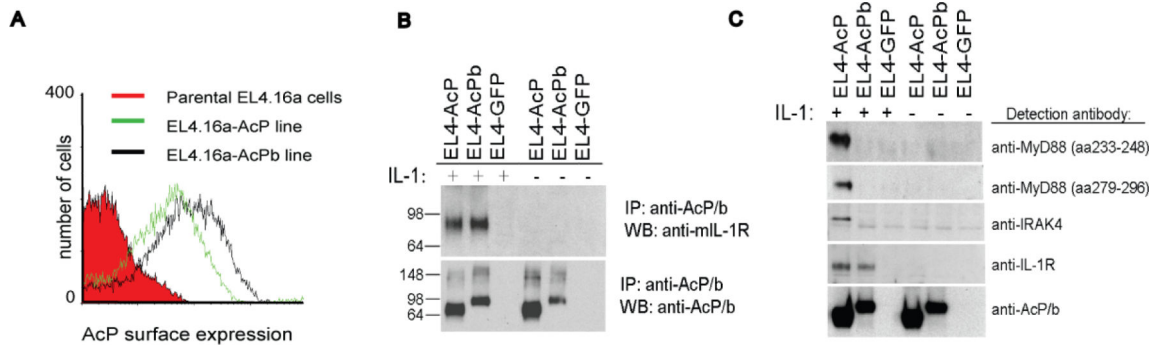
Figure 3. AcPb-mediated IL-1R and adapter recruitment
A, AcP surface expression on EL4.16a parental and stably-transfected cell lines utilizing an anti-AcP antibody that recognizes both forms of the receptor. **B**, EL4 lines were incubated with IL-1β (100 ng/ml) for 3 minutes then lysed and immunoprecipitated with a pan-AcP monoclonal antibody. Precipitations were analyzed by Western blot using either an anti-muIL-1R antibody or a pan-AcP antibody. Approximate molecular weights are indicated. **C**, Samples were stimulated and immunoprecipitated as in (B) and then adaptor protein recruitment was determined by Western blot with anti-MyD88 or IRAK4 antibodies, as indicated.
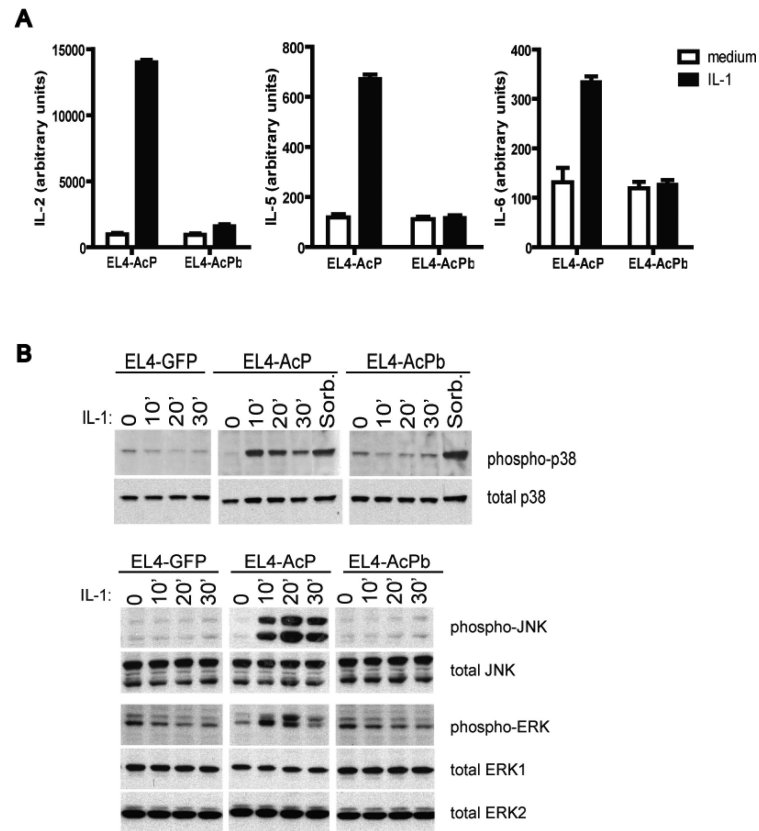
Figure 4. Signaling capacity of AcPb-reconstituted EL4 cells

A, EL4 lines were incubated for 24 hours in the presence of 300 ng/mL ionomycin and 100 pg/mL PMA plus or minus IL-1β (100 pg/mL), as indicated. Cytokine levels in the supernatants were quantified by Luminex (bead)-based multiplex assay and all assays were performed in triplicate. **B**, 2.0×10^7 cells were incubated with IL-1β(10 ng/mL) or 0.5M sorbitol at 37°C for various lengths of time and lysates (approximately 0.4×10^6 cell equivalents/lane) were probed by Western blot with total and phospho-specific antibodies against p38, JNK and ERK, as indicated.
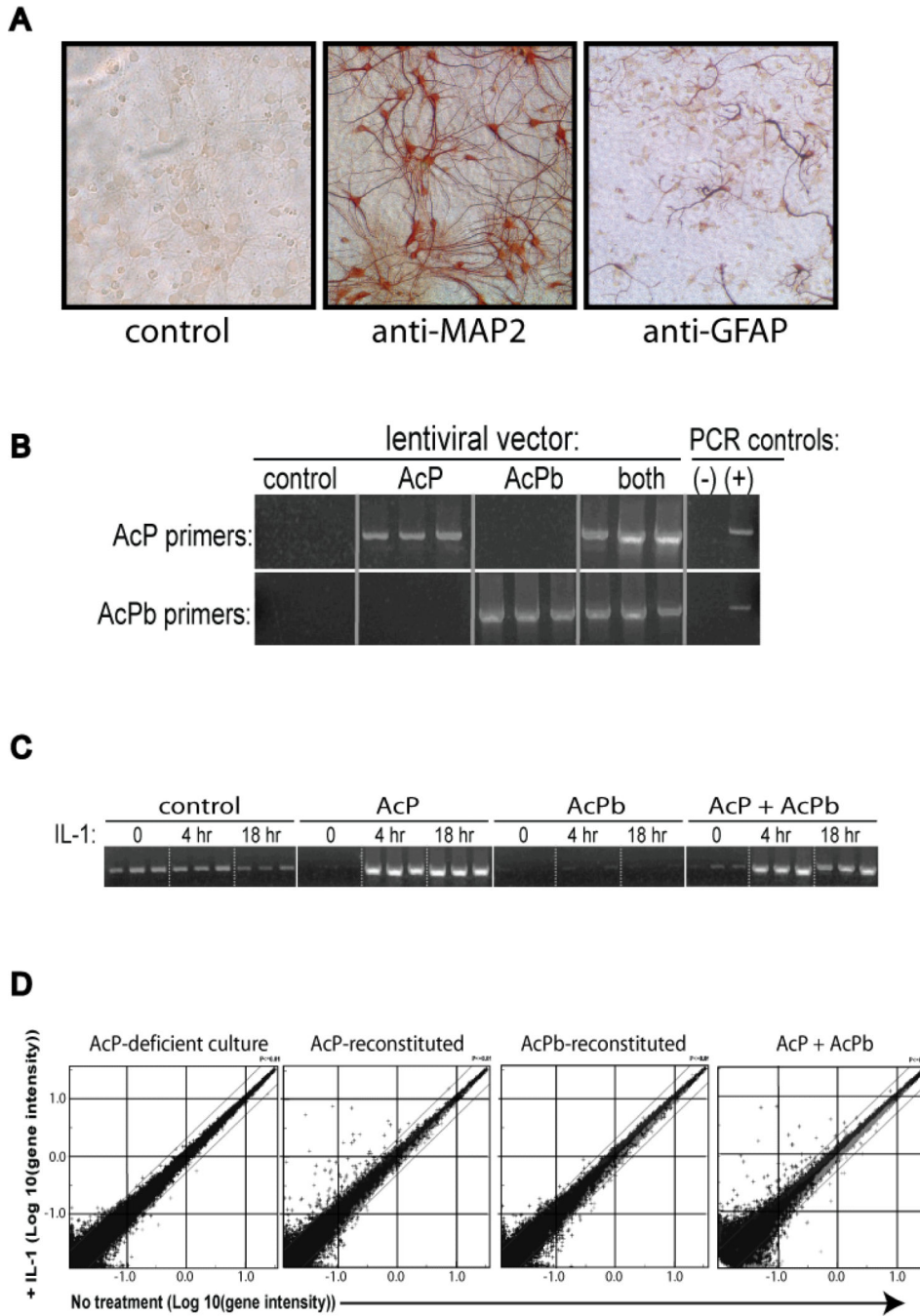
Figure 5. IL-1-induced responses in primary cortical neurons
A, C57BL/6 embryonic cortical neuron cultures were stained by immmunohistochemistry after 9 days of culture using antibodies that recognize either the neuronal-specific protein MAP-2 or the astrocyte-specific protein GFAP, as indicated. **B**, RT-PCR demonstrating specific expression of specific AcP isoforms in lentiviral vector-transduced neuronal cultures but not in non-transduced $AcP^{-/-}$ culture 2 days post transduction. **C**, RT-PCR detection of CCL2 transcript in transduced neuronal cultures stimulated for 4 or 18 hours with IL-1β (10 ng/mL), as indicated. **D**, Gene intensity profiles of AcP-deficient and AcP

isoform-reconstituted neuronal cultures (as indicated) stimulated with IL-1β (10 ng/mL) for 4 hours. RNA samples from triplicate stimulations for each cell population were used to hybridize a 45,000 probe set microarray as described in the methods.
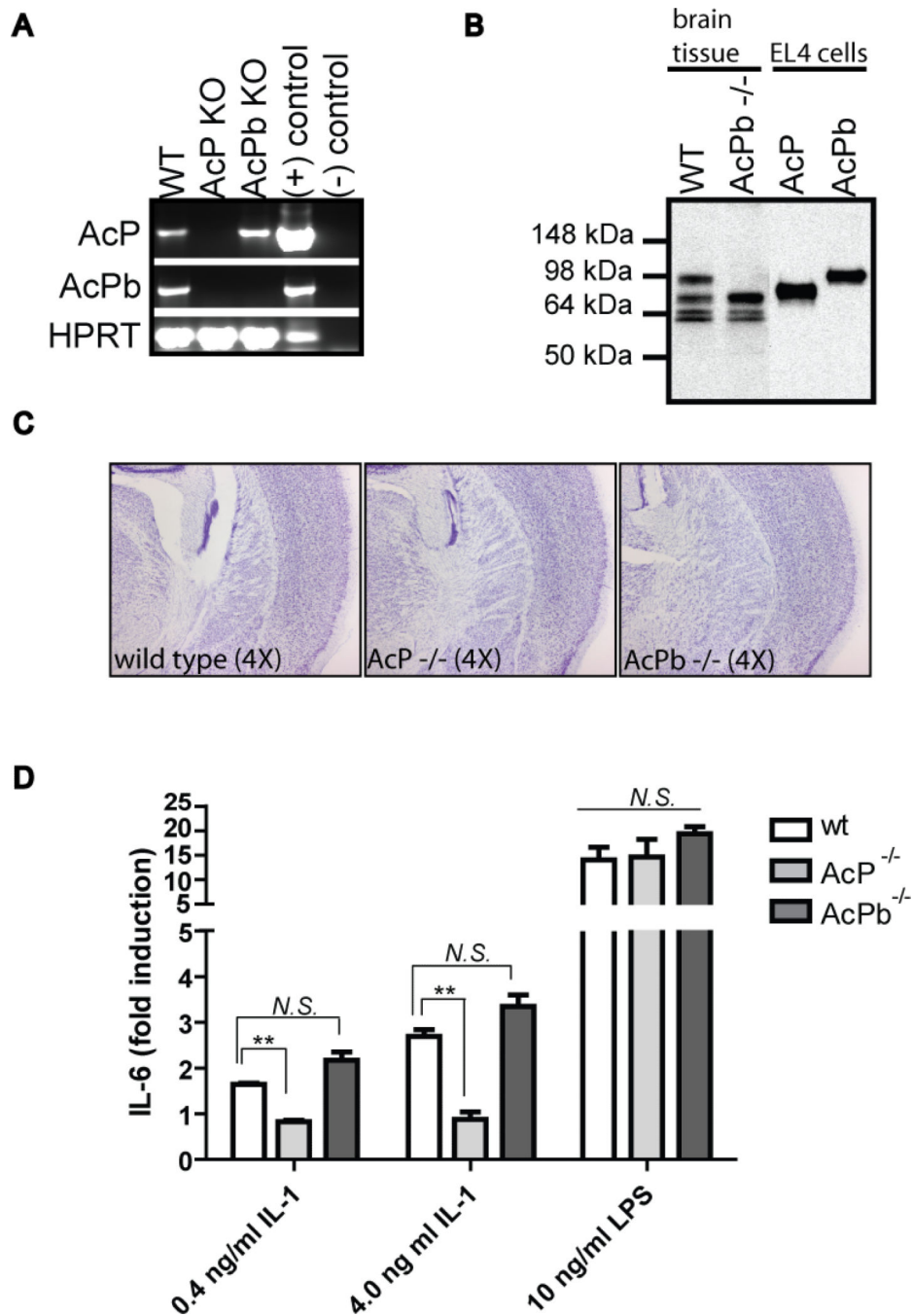
Figure 6. Generation of AcPb knockout mouse

AcPb-deficient animals were generated as described in the methods and as indicated in Figure 1. **A**, RT-PCR primers specific for AcP, AcPb or HPRT (as a control) were used to amplify cDNA generated from whole brain tissue from wild type, AcP$^{-/-}$ or AcPb$^{-/-}$ mice. Plasmid DNA for each cDNA was used as positive PCR controls and H$_2$O as a negative PCR control. **B**, immunoprecipitations of AcP- and AcPb-EL4 cell lysates or whole brain lysates from wild typeor AcPb$^{-/-}$ mice were performed with a pan-AcP antibody and analyzed by Western blot using a polyclonal anti-AcP antibody, as described in the methods.

C, Brains were collected from 10 week old mice and coronal plane sections were stained with Thionine- Nissl to reveal cell bodies and general morphology. Images are indicative of observations across the interval of sections from 3 age-matched mice per genotype. **D**, Splenocytes were isolated from wild type, AcP$^{-/-}$ or AcPb$^{-/-}$ mice and stimulated with IL-1β at the indicated concentrations. Supernatants were collected for determination of IL-6 levels after 48 hours. Results were generated using splenocytes from 3 individual mice per genotype and average fold induction is indicated **(N.S. = not significant, ** p<0.001).**
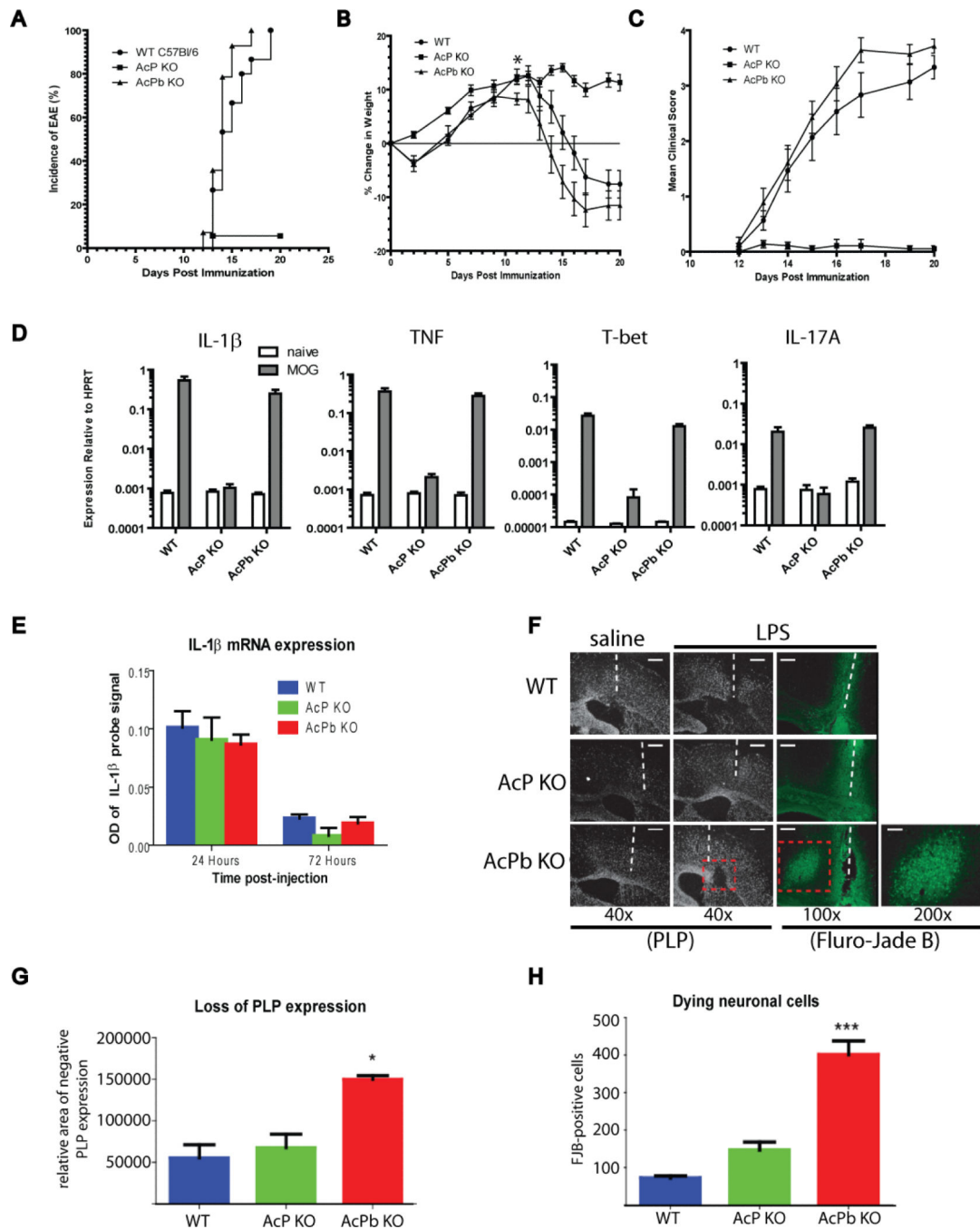
Figure 7. Effect of AcP and AcPb deletion in vivo: EAE (A-D) and acute LPS challenge in CNS (E-H)

Female C57Bl/6 wild type, AcP$^{-/-}$ or AcPb$^{-/-}$ mice (approximately 10 weeks old) were immunized s.c. with MOG$_{35-55}$ in CFA on day 0 to induce experimental autoimmune encephalomyelitis. Pertussis toxin (350 ng/mouse) in PBS was injected i.v. 48 hr after immunization. Animals were monitored, weighed, and scored for clinical disease every other day until disease was observed then daily thereafter. **A,** AcPb$^{-/-}$ mice (n=14) and wild type controls(n=15) had 100% disease incidence and a median day of onset of day 14 post immunization. AcP$^{-/-}$ mice (n=15) had significantly reduced disease incidence (5%, 1/18)

compared to wild type controls or AcPb$^{-/-}$ mice (p<0.0001, Logrank test). **B,** At day 11 post-immunization, the AcPb$^{-/-}$ mice had a statistically significant increase in weight loss compared to wild type controls (p<0.05, One way ANOVA, Tukey's post hoc test). **C,** AcPb$^{-/-}$ mice had a similar disease progression to that of wild type controls. AcP$^{-/-}$ mice had a significant reduction in mean clinical score on days 14-20 post-immunization (p<0.05, One way ANOVA, Tukey's post hoc test) and also suffered significant weight loss compared to wild type controls. **D,** RNA was extracted on day 20 post-immunization from spinal cords of 5 mice per strain, as indicated, and gene expression was profiled by real-time PCR. Average gene expression relative to HPRT is plotted for each gene. **E,** Mice (approximately 10 weeks old) were anesthetized and LPS (1.0 mg/mL) was injected intracerebrally over a one minute period. 3 days later, mice were deeply anesthetized and perfused, fixed brains were collected and processed as described in the methods. IL-1β mRNA was quantified following LPS administration by in situ hybridization. OD =optical density of IL-1β signal on radiographic film (*not shown*). Error bars represent variation among replicate animals per group. **F,** Proteolipid protein (PLP) in situ hybridization (black and white image) and Fluoro-Jade B (FJB) staining (cell bodies of degenerating neurons stain green) of brains 3 days post LPS administration. White dashed lines indicate location of injection tract and red dashed boxes indicate regions of localized PLP loss and FJB-positive neurons (also shown at 200× magnification from AcPb brain). The relative area of lost PLP expression (G) or the number of FJB-positive degenerating neurons (H) were quantified by ImageJ software. Results are expressed as mean ± SEM (* P < 0.05, *** P < 0.001), Data are representative of brains from either 3 or 4 individual mice per treatment group.

Table I

Two classes of AcP-dependent responses[1]

AcP-dependent responses unaffected by AcPb expression

Gene Name	Accession #	AcP (p value)	AcP+AcPb (p value)
Gbp2	NM_010260	**36.8 ± 13%** (0.0)	**38.5 ± 22%** (8.0E-24)
Ccl2, (MCP-1)	NM_011333	**14.1 ± 19%** (2.2E-17)	**13.6 ± 14%** (6.2E-27)
Cxcl2, (GRO beta)	NM_009140	**13.6 ± 21%** (5.4E-14)	**12.7 ± 29%** (3.0E-08)
Ptx3	NM_008987	**11.7 ± 9%** (0.0002)	**11.9 ± 13%** (0.0004)
Cxcl5, (LIX)	NM_009141	**10.0 ± 27%** (2.5E-07)	**8.8 ± 22%** (5.4E-09)
Egr2	NM_010118	**8.8 ± 14**%(2.0E-28)	**8.1 ± 13%** (2.8E-31)
Tlr2	NM_011905	**5.2 ± 13%** (7.9E-14)	**5.0 ± 14%** (5.9E-10)

AcP-dependent responses attenuated by AcPb expression

Gene Name	Accession #	AcP (p value)	AcP+AcPb (p value)
Atf3	NM_007498	**22.4 ± 37%** (1.6E-08)	**3.8 ± 19%** (0.00005)
Tnfrsf12a (Tweakr)	NM_013749	**39.3 ± 50%** (1.3E-12)	**1.9 ± 29%** (4.3E-08)
Cebpd	NM_007679	**12.7 ± 9%** (0.0)	**4.1 ± 14%** (1.8E-08)
Cp (Ceruloplasmin)	NM_001042611	**10.1 ± 14%** (5.1E-20)	**2.5 ± 22%** (0.01)
Fos	NM_010234	**2.9 ± 7%** (2.2E-13)	**1.5 ± 7%** (0.0008)

[1] Fold-change induction for each gene was measured in a ratio between sets of chips from triplicate samples of unstimulated and IL-1β-stimulated neuronal cultures with the Resolver log error converted to an average percentage. The p-value in parentheses is evaluated for the null hypothesis of no change due to stimulation, and is uncorrected for multiple testing. The second column is the IL-1 induced fold-change in AcP-deficient cells transduced with only the AcP vector, while the third column is for cells transduced with both AcP and AcPb vectors.